Sulphide mineralization at the E&L magmatic Ni-Cu-PGE deposit: Textural evidence for contamination, vapour saturation, fluid immiscibility, and metal remobilization

Matthew J. Brzozowski[1, a], and Katya Zaborniak[1]

[1] British Columbia Geological Survey, Ministry of Energy, Mines and Low Carbon Innovation, Victoria, BC, V8W 9N3
[a] corresponding author: Matthew.Brzozowski@gov.bc.ca

Abstract

The E&L magmatic Ni-Cu-PGE sulphide deposit is hosted by a small (~150 m wide near surface) stock with an apparent conduit geometry comprising varitextured gabbroic to wehrlitic rocks that crosscut the Nickel mountain gabbro and Middle Jurassic sedimentary rocks of the Hazelton Group. Sulphide mineralization occurs as disseminated, blebby, net-textured, and (semi-)massive sulphides. Several lines of textural evidence suggest that assimilation of sedimentary rocks likely played a role in the sulphide saturation history of the E&L magma including: 1) mixtures of gabbroic rock and sedimentary rock in which the two have diffuse boundaries; 2) an association of carbonate with sulphides; and 3) an association of sulphides with felsic patches in mafic rock. Considering that the sedimentary country rocks also contain sulphides, direct addition of S, either via bulk or selective assimilation, also likely played a role. Compound structures, which comprise segregated sulphide blebs with rims of fine-grained hydrous silicates (interpreted as former vapour bubbles), are common in the E&L deposit and imply that: 1) the E&L magma was volatile rich; 2) the magmas were emplaced at shallow crustal levels to permit volatile exsolution; and 3) sulphide liquid was transported upwards through the intrusive plumbing system. The inferred volatility of the E&L magmas is consistent with the common occurrence of orbicular textures in the gabbros. We interpret these orbicules to represent saturation of the E&L magma in H_2O and exsolution of a hydrous fluid phase, with the orbicules representing the melt and the interstitial material representing the immiscible fluid. After crystallization of the stock and generation of the primary sulphide mineralization, it is likely that metals were remobilized by the circulation of hydrothermal fluids. This inference is supported by: 1) the pervasive alteration of the rocks; 2) the replacement of chalcopyrite by pyrite; 3) the replacement of olivine ±pyroxene by an assemblage of hydrous silicates and sulphides; 4) the replacement of magnetite in magnetite-ulvöspinel-ilmenite intergrowths by an assemblage of hydrous silicates and sulphides; 5) the occurrence of sulphides in late-stage veins that crosscut the host rocks; and 6) the replacement of sulphides by magnetite (i.e., S loss).

Keywords: E&L deposit, Ni-Cu-PGE, magmatic sulphide, metal remobilization, mineral textures

1. Introduction

Nickel, Cu, Co, and the platinum-group elements (PGE) are considered critical metals because they are essential components of the batteries, electronics, and alloys that are needed for the transition to low-carbon emission economies. Intracontinental mafic-ultramafic intrusion-hosted magmatic sulphide deposits are the main global hosts of Ni and PGE resources (Mudd and Jowitt, 2014, 2022; Mudd et al., 2018) and are also significant hosts of Cu and Co. Although convergent-margin mafic-ultramafic intrusions are known to contain significant concentrations of PGE in Alaskan-type deposits (e.g., Tulameen, Nixon et al., 2018; Polaris, Milidragovic et al., 2021, 2023), they have generally not been considered good targets for other critical metals like Ni. Yet, several arc-related, mafic-ultramafic-hosted deposits exist globally that are base-metal enriched, including Giant Mascot and Turnagain in British Columbia (Scheel, 2004; Jackson-Brown et al., 2014; Manor et al., 2014, 2016), the Huangshan camp (Gao et al., 2013; Mao et al., 2015; Wang et al., 2021), Halatumiao (Sun et al., 2021), and Taoke (Zhang et al., 2021) in China,

Aguablanca in Spain (Pina et al., 2010), Duke Island in Alaska (Thakurta et al., 2008; Stifter et al., 2016), Ferguson Lake in Nunavut (Acosta-Góngora et al., 2018), and Portneuf-Mauricie in Quebec (Sappin et al., 2009). Although the fundamental mechanisms by which arc-related magmatic sulphide deposits form are the same as in intracontinental settings (i.e., mantle partial melting, sulphide saturation, enrichment of sulphide liquid in metal by sulphide liquid-silicate melt interaction, and concentration of sulphide liquid; Naldrett, 2010), several aspects of their genesis remain poorly constrained, including mantle source composition, sulphide saturation and metal enrichment mechanisms, and the nature of the critical mineral hosts (e.g., sulphide, chromite, platinum-group minerals, and alloys). These ambiguities reflect that, relative to deposits in intracontinental settings (e.g., Noril'sk, Naldrett, 1992; Duluth, Lee and Ripley, 1995; Jinchuan, Li et al., 2005; Eagle, Ding et al., 2011; Voisey's Bay, Lightfoot et al., 2012; Marathon, Brzozowski et al., 2020), little research has been done on this subtype of the Ni-Cu-PGE sulphide system.

In British Columbia, Ni and the PGE are almost exclusively

65

Geological Fieldwork 2023, British Columbia Ministry of Energy, Mines and Low Carbon Innovation, British Columbia Geological Survey Paper 2024-01

hosted by mafic-ultramafic intrusions, many of which are Cu-bearing. Nickel-Cu-PGE deposits in British Columbia are principally hosted by Alaskan-type and other mafic-ultramafic intrusions in the Quesnel and Stikine terranes (Fig. 1; Nixon et al., 2020). These deposits exhibit a range of sulphide contents and host a variety of metals; some are endowed in the PGE, but have limited sulphide (e.g., Tulameen, Polaris), whereas others are endowed in base metals and are sulphide rich (e.g., Giant Mascot, Turnagain, E&L). The cause of this mineralogical and geochemical diversity remains poorly understood because

the mechanisms leading to the formation of many of these deposits have not been well studied. To address this deficiency and improve our understanding of convergent margin-related magmatic Ni-Cu-PGE sulphide deposits, we initiated a multi-year project of the E&L property in northwestern British Columbia (Fig. 1) in the traditional lands of the Tahltan First Nation. In collaboration with Garibaldi Resources Corp., the goals of this project are to: 1) determine the age of the E&L stock; 2) establish the magmatic source(s) of the E&L pluton; 3) assess the genetic relationship between the mineralized E&L
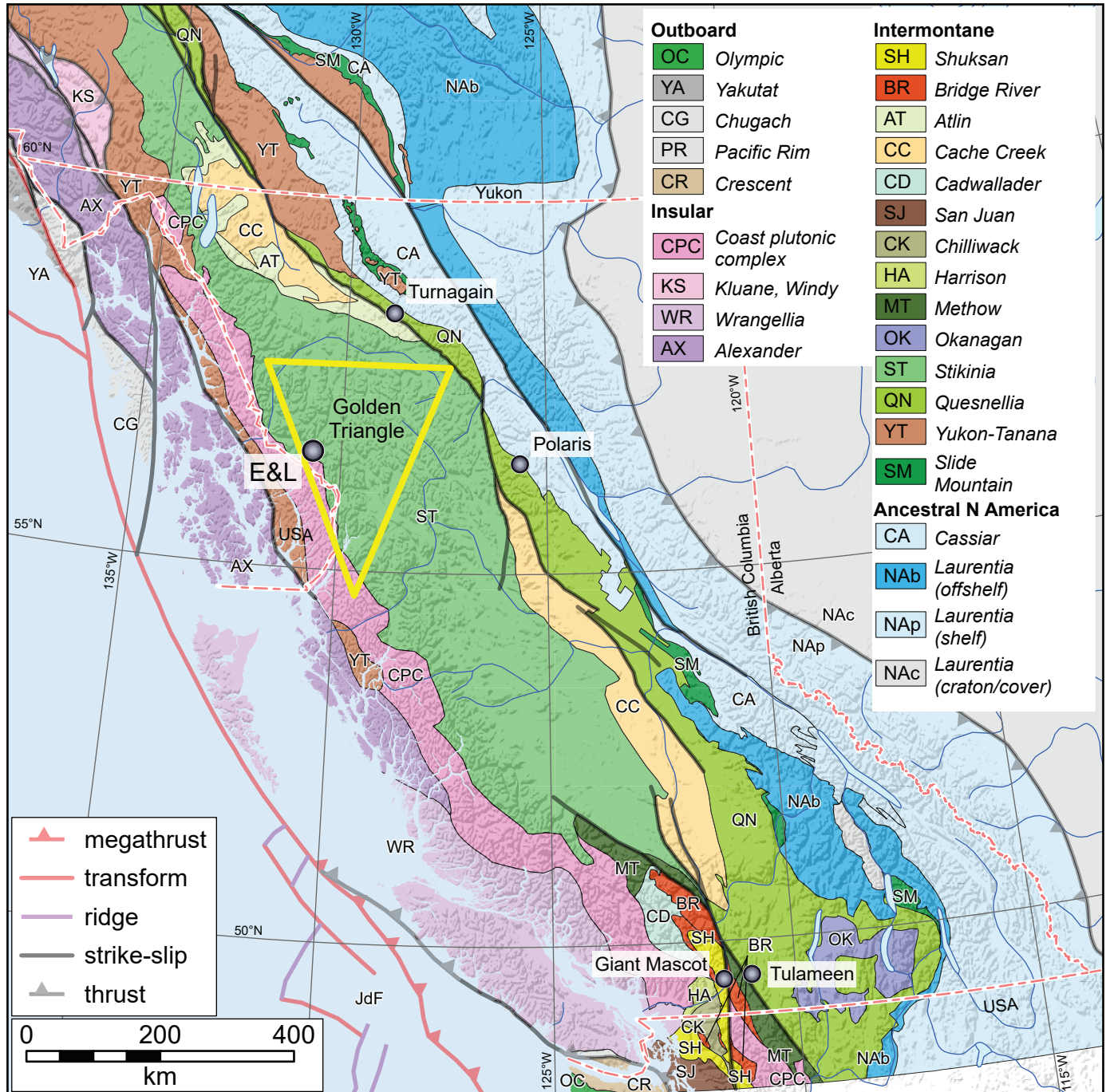
Fig. 1. Location of the E&L property in Stikine terrane. Terranes modified from Colpron (2020).

66

Geological Fieldwork 2023, British Columbia Ministry of Energy, Mines and Low Carbon Innovation, British Columbia Geological Survey Paper 2024-01

pluton and the barren country rocks of the Nickel mountain gabbro that it was emplaced into; 4) consider sulphide saturation and metal enrichment mechanisms and the possible role of Hazelton Group country rock assimilation; and 5) determine the hosts to the critical metals. In this initial report, we summarize the geometry of the E&L deposit based on drilling by Garibaldi Resources Corp., document the lithological, mineralogical, and textural variations observed throughout the E&L deposit based on examination of drill core samples, and provide preliminary interpretations into what these variations may indicate about the processes that generated the deposit.

2. Regional setting

The E&L property is in northern Stikinia, the northwest-trending terrane extending for about 1000 km along the length of the Canadian Cordillera and containing prominent Carboniferous to Middle Jurassic island arc-related volcano-sedimentary successions and allied intrusive rocks (Fig. 1; Nelson et al., 2013, 2022). The property is in the 'Golden Triangle', the popular name for a loosely defined area remarkably well-endowed with economic metals, with more than 150 deposits that have been mined since the end of the 19th

century, many proposed mines, numerous advanced exploration projects, and two current mines (Red Chris, Brucejack, Fig. 2; British Columbia Geological Survey, 2023). The main rock units in the region include the Stikine assemblage (lower Paleozoic), Stuhini Group (Upper Triassic), and the Hazelton Group (Upper Triassic to Middle Jurassic), and the alkalic to calc-alkaline intrusive rocks spatially and temporally related to these units. These units are covered by the Bowser Lake Group (Middle Jurassic) and cut by Cretaceous to Eocene rocks of the Coast Plutonic complex (Fig. 2).

3. Local geology

In the study area, the geology comprises mudstone, siltstone, and carbonate-rich rocks of the Spatsizi Formation (for Hazelton Group stratigraphy see Nelson et al., 2018) that were intruded by four 100-m wide plugs and one 800-m wide stock (Hancock, 1990), which Garibaldi Resources Corp. refer collectively to as the 'Nickel mountain gabbro complex'. These plugs and stocks comprise equigranular Fe-Ti oxide-bearing gabbro and minor norite that intruded Hazelton Group volcano-sedimentary rocks at ca. 180 Ma (Fig. 3; Hancock, 1990; Chamberlain, unpublished zircon CA-TIMS U-Pb data,
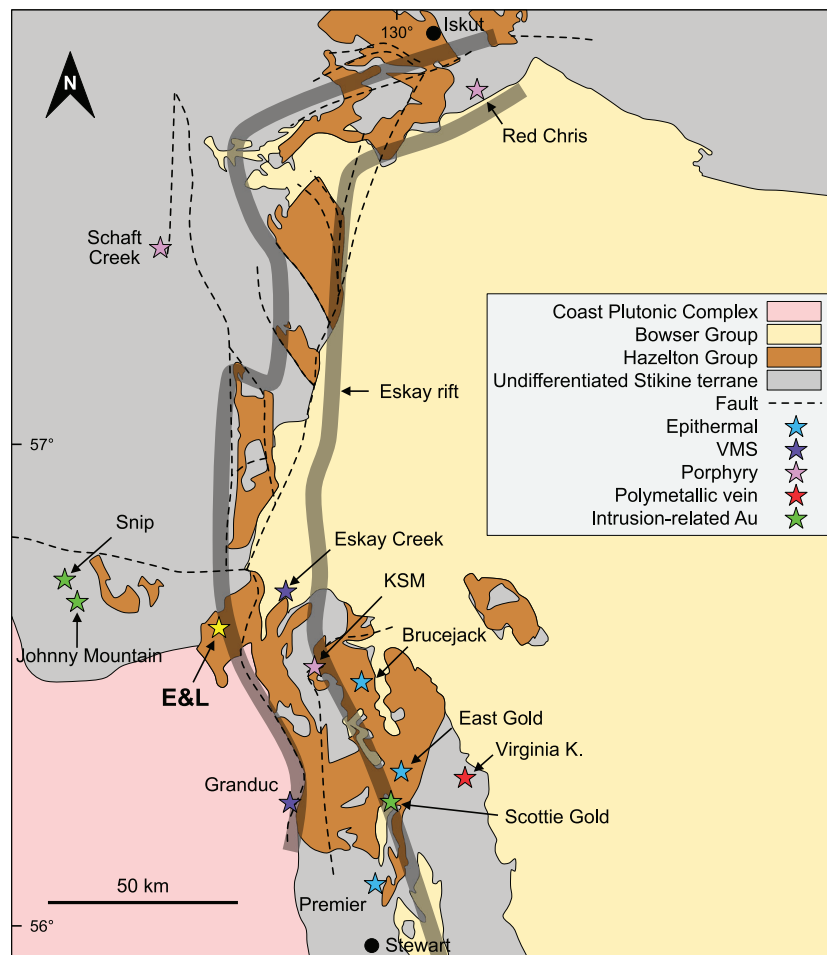
Fig. 2. Generalized geology of the Iskut River region showing the location of the E&L magmatic sulphide deposit, producing mines (Red Chris, Brucejack), and past-producing base metal deposits. Modified after Nelson et al. (2018). Outline of Eskay rift from Gagnon et al. (2012).

67

Geological Fieldwork 2023, British Columbia Ministry of Energy, Mines and Low Carbon Innovation, British Columbia Geological Survey Paper 2024-01
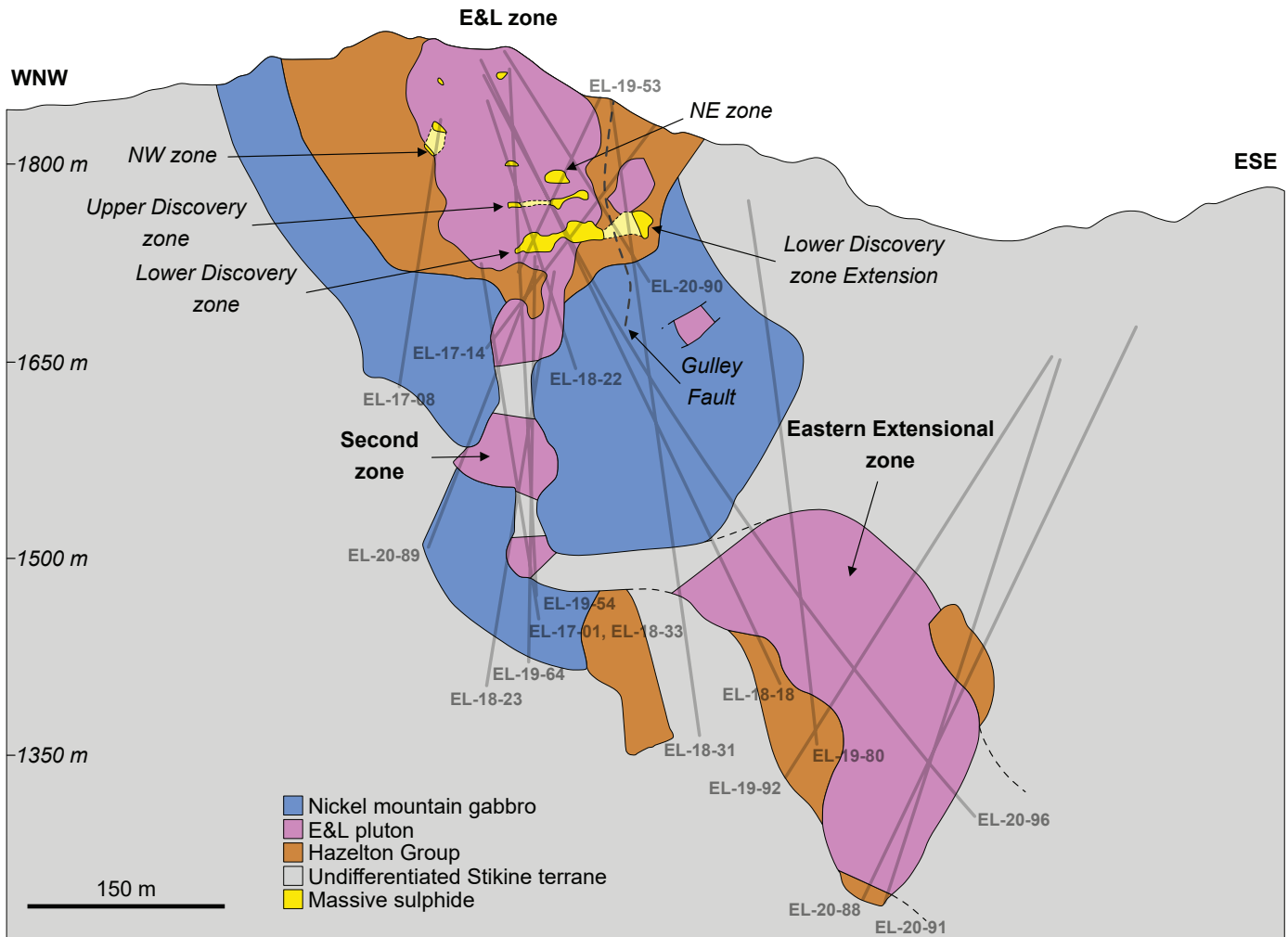
Fig. 3. Schematic cross-section of the E&L deposit illustrating the conduit-like geometry of the E&L pluton and its relationship to older gabbros and sedimentary rocks of the Hazelton Group, and the locations of massive sulphide orebodies. Modified after Hanson et al. (2022).

cited in Vandenburg, 2020). The E&L stock is a relatively small base- and precious-metal-mineralized deposit which, based on drilling data, appears to have a conduit geometry (~150 m wide near surface, ~250 m wide at depth) and to have intruded the Nickel mountain gabbro and sedimentary rocks (mudstones, siltstones, and carbonate-rich rocks) of the Spatsizi Formation (Fig. 3) on the southwestern flank of Nickel mountain. The stock outcrops at the top of Nickel mountain at ~1900 m asl and extends to a depth of at least 1200 m asl (Fig. 3). It comprises orbicular to varitextured Fe-Ti oxide-bearing olivine melagabbro, gabbronorite, and gabbro, with lesser wehrlite (Vandenburg, 2020). Rocks of the Nickel mountain gabbro and the E&L stock contain propylitic and potassic alteration assemblages and were metamorphosed to greenschist facies during regional ca. 110 Ma deformation (Alldrick et al., 1987; Hancock, 1990). The rocks lack macroscopic textural evidence for deformation. Of the gabbroic rocks in the area, only those of the E&L stock host significant magmatic Ni-Cu-PGE mineralization in the form of disseminated, net-textured, and semi-massive to massive pyrrhotite, pentlandite,

and chalcopyrite (Vandenburg, 2020). Based on whole-rock primitive mantle-normalized trace-element patterns, Nb-Ta depletion, and decoupled large ion lithophile and high field strength element signatures, Vandenburg (2020) suggested that the rocks of the Nickel mountain gabbro and E&L stock crystallized from subduction-derived magmas that originated from distinct mantle sources. For the E&L gabbros, Vandenburg (2020) suggested that the elevated forsterite contents of olivine (Fo_{78-84}) and low Ni-Co contents indicated they crystallized from a high-Mg parent magma, and that sulphide saturation likely occurred before olivine crystallization.

4. Deposit geology

Based on drilling data (Fig. 3), the E&L deposit appears to represent a conduit-type magmatic Ni-Cu-PGE sulphide system. The deposit has been informally subdivided by Garibaldi Resources Corp. into: 1) the E&L zone, which is exposed on Nickel mountain and extends to a depth of ~1700 m asl; 2) the Eastern Extensional zone, which extends to depths greater than at least 1500 m asl; and 3) the Second zone, which

68

Geological Fieldwork 2023, British Columbia Ministry of Energy, Mines and Low Carbon Innovation, British Columbia Geological Survey Paper 2024-01

connects these zones and has a thin (~50-100 m wide), pipe-like morphology (Fig. 3). Mineralization occurs within orbicular and taxitic gabbros of the E&L stock and comprises a textural spectrum of sulphides ranging from disseminated and blebby to net-textured to massive sulphide (pyrrhotite>chalcopyrite> pentlandite ±sphalerite, pyrite, violarite; Vandenburg, 2020). Disseminated and blebby sulphide mineralization contains 1-25 vol.% sulphide, with higher abundances in olivine-rich gabbros that have well-developed orbicules. Texturally, the sulphides may be interstitial to silicate and oxide minerals or occur as blebs. Net-textured sulphide (5-20 vol.%) represents a (semi-)continuous matrix of sulphide in a framework of olivine, clinopyroxene, and plagioclase. Semi-massive sulphide (20-90 vol.%) is at the boundaries of massive sulphide orebodies and commonly contains inclusions of recrystallized Hazelton Group country rock. Several massive sulphide (>90 vol.%) orebodies have been identified: Upper Discovery zone, Lower Discovery zone (largest), Northwest zone, and Northeast zone (Fig. 3). Many of the massive sulphide orebodies have been deformed, which may have remobilized some of the chalcopyrite. In terms of metal tenors, Cu, Pt, Pd, and Au concentrations are typically greatest at the tops of the massive sulphide orebodies, Rh concentrations are typically greatest in the central portion of the orebodies, and Ni concentrations are generally uniform (Lightfoot, pers. comm., 2023). Platinum-group minerals are uncommon, occurring primarily as tellurides (<1 vol.%; Vandenburg, 2020).

5. Sample descriptions

We collected five outcrop samples and 309 core samples from nine holes drilled by Garibaldi Resources Corp. between 2017 and 2020 at Nickel mountain. Representative samples were selected for thin section examination, and for future geochemical and isotopic analyses.

5.1. Hand samples
5.1.1. E&L stock

Variably mineralized samples of leucogabbro, melagabbro, olivine gabbro, varitextured gabbro, wehrlite, and mixtures of these rocks with sedimentary rock were collected from the E&L stock, including samples from the E&L zone (n=58), the Second zone (n=18), and the Eastern Extension zone (n=40). These samples largely consist of variable proportions of medium- to coarse-grained olivine, pyroxene, and plagioclase. Mineralization comprises disseminated (Fig. 4a), blebby (Fig. 4b), semi-massive, (Fig. 4c), and massive sulphide (Fig. 4d), mainly pyrrhotite, pentlandite, and chalcopyrite. Blebby sulphides are typically segregated into pyrrhotite-pentlandite-rich and chalcopyrite-rich portions, the latter with rims of fine-grained hydrous silicates (Fig. 4b). Some disseminated and blebby sulphides display rims of pyroxene (Fig. 4e). Many samples contain cm-scale orbicules with variable proportions of plagioclase, olivine, and clinopyroxene, an assemblage similar to the interstitial rock (Fig. 4f). Some of these orbicules exhibit crude zoning defined by modal

variations in the proportions of olivine+pyroxene versus plagioclase, with a mafic core and plagioclase-rich rim (Fig. 4f), and some have coarse centres surrounded by finer grained rims (Fig. 4f). A smaller variety of these orbicules is also common in many samples; these circular features also typically display a core of mafic minerals and a rim of plagioclase (Fig. 4g). The regions interstitial to the orbicules appear to be more mafic in composition and coarser grained; sulphides seem to largely be restricted to regions interstitial to the orbicules, but fine-grained sulphides also occur within them (Figs. 4f, g). Where orbicules touch one another, contacts are deformed, the finer grained cores are preserved, and the orbicules retain their individual identities rather than merging into a single body (Fig. 4g). Although most of the samples are mafic, comprising variably altered plagioclase, pyroxene, and olivine, a few samples contain felsic patches (Figs. 4c, h). The diffuse boundaries between Hazelton Group material and gabbro (Fig. 4i), and possibly these felsic patches, indicate interaction between mafic magma and sedimentary country rock. An additional 12 samples of what is potentially E&L gabbro were obtained from an exploratory hole drilled below glacial ice. These samples lack orbicules and significant sulphides, most of which are fine disseminations (Fig. 4j).

5.1.2. Nickel mountain gabbro and country rock

Samples from the Nickel mountain gabbro (n=80) include leucogabbro, melagabbro, and olivine gabbro. These gabbroic rocks are equigranular assemblages of variably altered plagioclase, pyroxene, olivine, and magnetite, with plagioclase-rich (Fig. 4k) and plagioclase-poor variants (Fig. 4l). In general, the subhedral-euhedral plagioclase ±magnetite and common interstitial pyroxene suggest that plagioclase and magnetite crystallized before pyroxene. Although not significantly mineralized, a few samples contain sparse fine-grained sulphide and, rarely, semi-massive sulphide (Fig. 4m). The most notable feature of the siltstone and mudstone samples from the Spatsizi Formation (n=42), is the presence of sulphides, typically pyrite (Figs. 4n, o).

5.2. Thin section descriptions

The gabbroic rocks of both the E&L stock and Nickel mountain gabbro consist mainly of olivine, pyroxene, and plagioclase that display an ophitic texture, with pyroxene interstitial to euhedral laths of plagioclase and rounded olivine crystals. The inferred order of crystallization is olivine, plagioclase, and pyroxene. All of the rocks are extremely altered, with primary silicates in some samples completely replaced by hydrous silicates. In general, olivine is the most intensely altered, commonly appearing as hydrous silicate aggregate pseudomorphs. Plagioclase and pyroxene are variably altered. The olivine has been serpentinized and replaced by sulphides, plagioclase has been sericitized and chloritized, and pyroxene was chloritized or uralitized and replaced by sulphides.

Mineralization in the E&L stock occurs as disseminated, blebby, net-textured, and semi-massive sulphides comprising

69

Geological Fieldwork 2023, British Columbia Ministry of Energy, Mines and Low Carbon Innovation, British Columbia Geological Survey Paper 2024-01
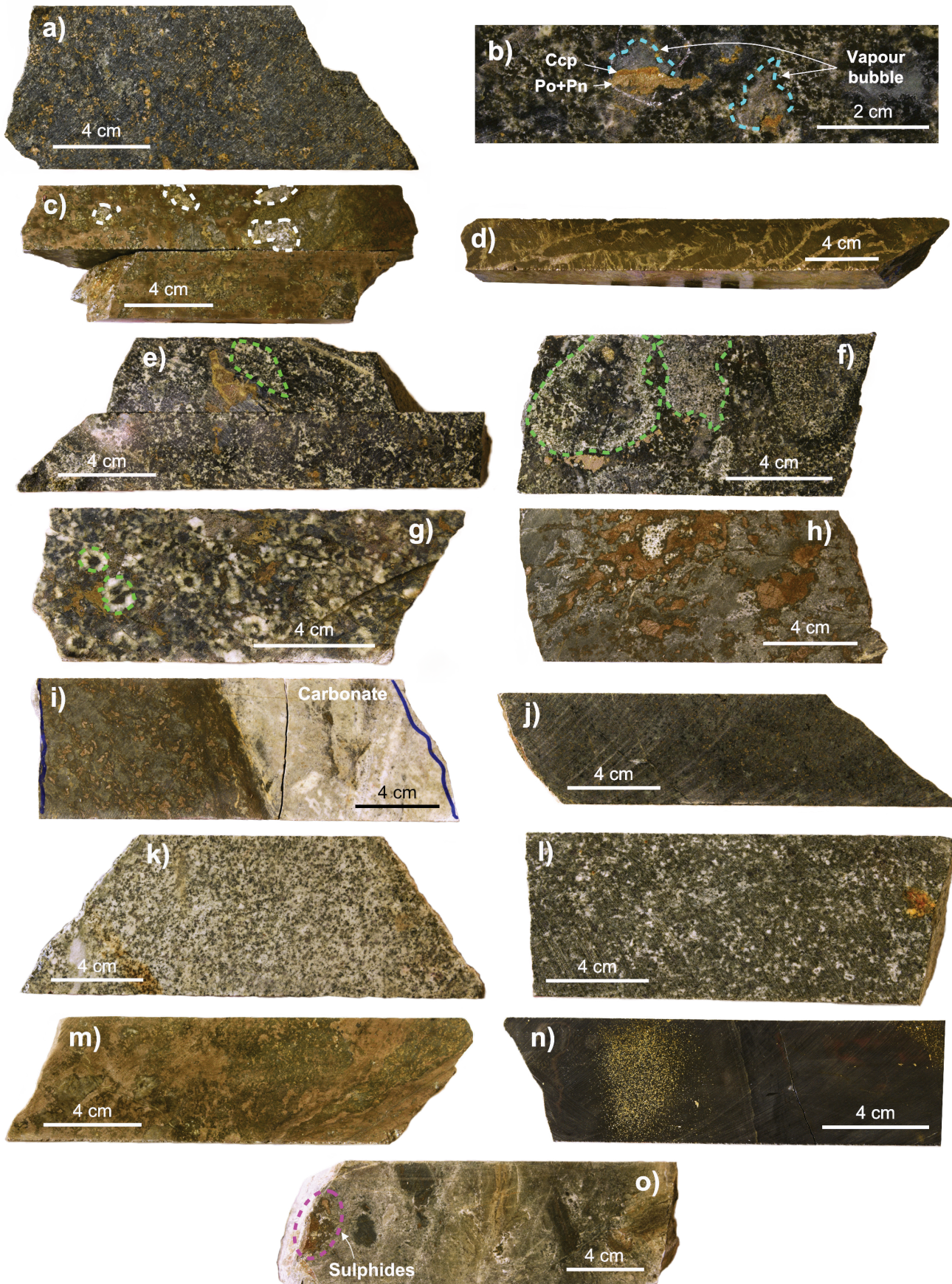
Fig. 4. See opposite page for caption.

70

Geological Fieldwork 2023, British Columbia Ministry of Energy, Mines and Low Carbon Innovation, British Columbia Geological Survey Paper 2024-01

Fig. 4. Continued. Images of representative drill core samples of (a-j) E&L gabbro and sulphide mineralization, (k-m) Nickel mountain gabbro, and (n-o) Hazelton Group (Spatsizi Formation) sedimentary rock. **a)** Disseminated sulphide mineralization in E&L gabbro. **b)** Blebby sulphide mineralization in E&L gabbro. Note the segregation of the sulphide bleb into Fe-rich and Cu-rich portions, the latter of which is surrounded by a fine-grained assemblage of hydrous minerals. **c)** Semi-massive sulphide mineralization with felsic patches. **d)** Massive sulphide mineralization showing loop texture (rounded aggregates of pyrrhotite surrounded by pentlandite and chalcopyrite). **e)** Blebby sulphide mineralization in E&L gabbro; the sulphide bleb is surrounded by pyroxene. **f)** Varitextured gabbro with well-defined orbicules (outlined by green dashed lines). The sulphides are largely interstitial to the orbicules. **g)** Varitextured gabbro with small-scale orbicular features; two are highlighted by green dashed lines. Sulphides are interstitial to the orbicular features. **h)** Semi-massive sulphide mineralization in rock comprising a mixture of mafic material with more silicic material. Sulphides are associated with the more felsic-rich domains. **i)** Disseminated sulphide mineralization in a sample of E&L gabbro in contact with sedimentary country rock. **j)** Disseminated sulphide mineralization in gabbroic rock from the exploratory drill hole under the glacier on top of Nickel mountain. **k)** Plagioclase-rich Nickel mountain gabbro. **l)** Plagioclase-poor Nickel mountain gabbro. **m)** Nickel mountain gabbro hosting semi-massive sulphide mineralization. **n)** Siltstone of the Spatsizi Formation containing fine-grained, disseminated pyrite. **o)** Mudstone of the Spatsizi Formation containing blebby sulphides (highlighted by purple dashed circle). The teal dashed lines delineate features interpreted as former vapour bubbles, the white dashed lines highlight felsic patches, and the green dashed lines are orbicules.

pyrrhotite, chalcopyrite, pentlandite, and pyrite; cubanite, violarite, and troilite are rare. Where pyrite is absent, the order of sulphide abundance is generally pyrrhotite>chalcopyrite ≥pentlandite (Fig. 5a). However, pyrite may make up a significant portion of the sulphide assemblage, with some samples containing predominantly pyrite (Fig. 5b). Given that pyrite is rarely a primary sulphide in magmatic deposits because sulphide liquids typically do not achieve high enough S/metal ratios (Naldrett et al., 1967; Kellerud et al., 1969; Craig, 1973; Piña et al., 2016), it is likely that pyrite is hydrothermal in origin, as described by Brzozowski et al. (2023) for the Current deposit in the Midcontinent Rift. The sulphide assemblage at E&L may, therefore, be broadly grouped into two categories: primary, lacking abundant pyrite, and secondary, with abundant pyrite. There appears to be no systematic variation in sulphide mineralogy across different parts of the deposit.

The primary sulphide assemblage comprises pyrrhotite, chalcopyrite, and pentlandite that exhibit sharp, rounded inter-grain boundaries (Fig. 5a), a mineralogical and textural assemblage typical of sulphides that crystallized from a sulphide liquid. Generally, pyrrhotite is the predominant sulphide, with chalcopyrite occurring along its periphery (although locally as streaks within pyrrhotite). Pentlandite occurs as aggregates near contacts between pyrrhotite and chalcopyrite, as grains within pyrrhotite (Fig. 5a), and locally as flames in pyrrhotite. The secondary sulphide assemblage comprises pyrite ±pyrrhotite, chalcopyrite, and pentlandite. Pyrite typically occurs as porous aggregates of fine-grained crystals spatially associated with mineralogically variable assemblages of pyrrhotite-chalcopyrite-pentlandite (Fig. 5b) or as isolated clusters (Fig. 5c). Where spatially associated with other sulphides, pyrite typically appears to have replaced pyrrhotite (Fig. 5b).

Regardless of whether primary or secondary, the sulphides are almost always spatially associated with hydrous silicates reflecting the pervasive alteration of the rocks; in some assemblages, the hydrous silicates also protrude into the sulphides. Where sulphides are associated with what we interpret as vapour bubbles (e.g., Fig. 4b), the vapour bubble now comprises an assemblage of hydrous silicates (Fig. 5d). Although not as common, some sulphide assemblages may also contain carbonate, either within the assemblage or along its periphery (Fig. 5e). Additionally, pyrrhotite in both assemblage types can exhibit undulose extinction in cross-polarized reflected light, with some pyrrhotite grains displaying distinct flaser texture (Fig. 5f) or 120° dihedral angles (Fig. 5g). In most samples, fine-grained specks of sulphide occur throughout the alteration assemblages. A specific example of this sulphide-alteration association are the intensively altered olivine grains that commonly contain variable amounts of fine-grained pyrrhotite (±chalcopyrite and pentlandite), with some of the olivine grains being almost completely pseudomorphed by sulphide (Fig. 5h). Although less common, an assemblage of hydrous silicates+chalcopyrite has also been observed as partial pseudomorphs of altered primary silicates (Fig. 5i). Similarly, where Fe-Ti oxide minerals (i.e., magnetite-ulvöspinel-ilmenite intergrowths) have been altered, the magnetite interstitial to relics of the lamellae has been replaced by hydrous silicates+sulphides (Fig. 5j). Although uncommon, some sulphides occur within veinlets (Fig. 5k). Similarly uncommon, some sulphide assemblages are rimmed by magnetite (Fig. 5l).

6. Discussion
6.1. Sulphide saturation via contamination?

Magmas emplaced at crustal levels are typically undersaturated in sulphide because the sulphur content at sulphide saturation increases as pressure decreases (Mavrogenes and O'Neill, 1999). The formation of magmatic sulphide deposits, therefore, requires some additional process(es) to cause the parental magmas to become saturated in sulphide and segregate a sulphide liquid, which then scavenges and concentrates base and precious metals. Achieving sulphide saturation is problematic in subduction zones because the magmas are oxidized and sulphur may be present as sulphate (SO_4^{2-}) rather than sulphide (S^{2-}) anions (Jugo, 2004, 2009), requiring reduction. Several processes have been proposed to assist magmas in becoming saturated in sulphide (e.g., Ripley and Li, 2013) including: 1) closed-system fractional crystallization; 2) magma mixing; 3) decrease in magma fO_2; and 4) addition of externally derived S and/or Si. Ripley and Li (2013) evaluated each of these processes and concluded that direct addition of externally derived S is the most viable for generating sufficient

71

Geological Fieldwork 2023, British Columbia Ministry of Energy, Mines and Low Carbon Innovation, British Columbia Geological Survey Paper 2024-01
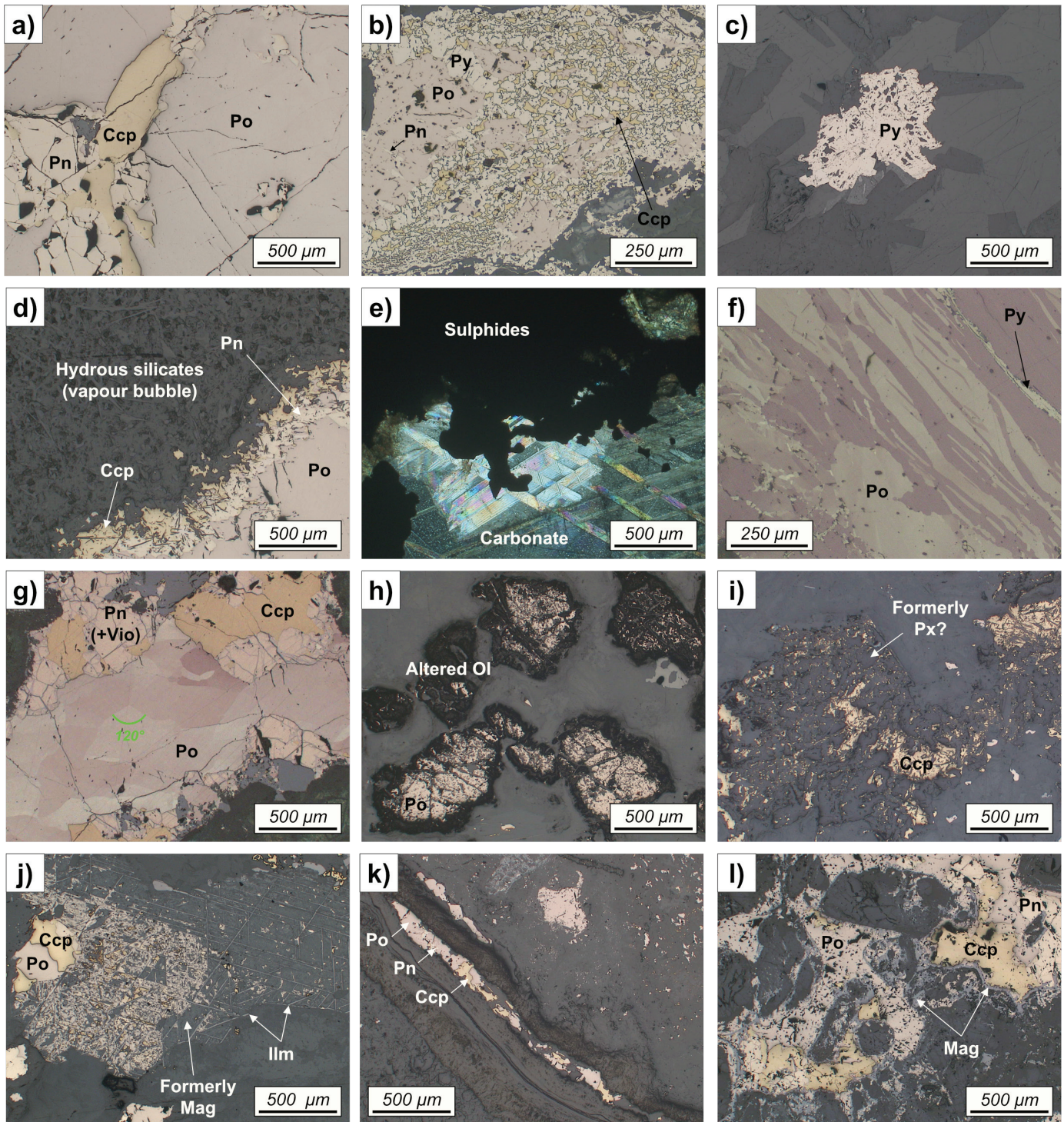
Fig. 5. Photomicrographs of representative sulphide textures in the E&L deposit; (a-d) and (h-l) are in reflected light, e) is in cross-polarized transmitted light, and (f-g) are in cross-polarized reflected light. **a)** A magmatic sulphide assemblage comprising pyrrhotite-pentlandite-chalcopyrite. **b)** An altered sulphide assemblage comprising pyrrhotite-pentlandite-chalcopyrite-pyrite, with pyrite forming aggregates. **c)** An aggregate of pyrite grains isolated from other sulphides. **d)** A magmatic sulphide assemblage comprising pyrrhotite-pentlandite-chalcopyrite adjacent to a rounded hydrous silicate assemblage that is interpreted as a former vapour bubble. **e)** Carbonate and hydrous silicates adjacent to sulphides. **f)** Pyrrhotite with flaser texture. **g)** A magmatic assemblage of pyrrhotite-pentlandite-chalcopyrite in which the pyrrhotite occurs as an aggregate of grains that exhibit dihedral angles. **h)** Olivine that has been partially to completely replaced by hydrous silicates and pyrrhotite. **i)** Pyroxene(?) replaced by an assemblage of hydrous silicates and chalcopyrite. **j)** A grain of Fe-Ti oxide (magnetite+ilmenite) in which the magnetite has been replaced by an assemblage of hydrous silicates and sulphides. **k)** A late-stage vein containing pyrrhotite, pentlandite, and chalcopyrite. **l)** A magmatic sulphide assemblage of pyrrhotite, pentlandite, and chalcopyrite rimmed by magnetite.
Abbreviations: Po – pyrrhotite, Pn – pentlandite, Ccp – chalcopyrite, Py – pyrite, Vio – violarite, Ilm – ilmenite, Ol – olivine, Mag – magnetite.

72

Geological Fieldwork 2023, British Columbia Ministry of Energy, Mines and Low Carbon Innovation, British Columbia Geological Survey Paper 2024-01

sulphide liquid to form economic Ni-Cu-PGE deposits. Below we make a preliminarily assessment of the saturation mechanisms that may have operated in the E&L deposit using textural observations.

Saturation of the E&L magma via closed-system fractional crystallization of the stock seems unlikely for two reasons. First, the geometry of the E&L deposit appears to define an open, conduit-like system, and so the cumulate rocks likely crystallized from multiple batches of magma rather than from a single, evolving magma. This interpretation is consistent with what appears to be two magma chambers in the E&L intrusive system that are interpreted to be connected by a pipe-like body (Fig. 3) similar to, for example, the Voisey's Bay (Evans-Lamswood et al., 2000; Ripley and Li, 2011), Noril'sk (Barnes et al., 2015), and Eagle (Ripley and Li, 2011) deposits. Furthermore, the elevated metal contents of the E&L deposit, and other volumetrically small sulphide deposits, require larger volumes of magma than represented by the stock itself (Campbell and Naldrett, 1979; Naldrett, 1989, 1992, 1999; Arndt et al., 2005). Second, sulphide saturation via crystallization generates small volumes of sulphide liquid late in the crystallization history of a magma (after up to 40% crystallization, Ripley and Li, 2013; Mungall, 2014). Such late saturation is inconsistent with the net-textured and (semi-) massive sulphide orebodies (Figs. 3, 4c, d, m) at E&L, which would have required relatively early saturation to prevent sulphide liquid from being completely trapped in the cumulate pile. The high volumes of sulphide at E&L are inconsistent with magma mixing, which generally produces only small amounts of sulphide (Ripley and Li, 2013), and textural evidence of mixing is lacking. Decreasing the fO_2 of a magma, although not necessarily important to the saturation history of intracratonic magmatic systems where fO_2 values are lower than fayalite-magnetite-quartz (FMQ) buffer (Mavrogenes and O'Neill, 1999; O'Neill and Mavrogenes, 2002), may be important to the saturation histories of arc-related magmas where both sulphide and sulphate can coexist (FMQ to FMQ+2; Jugo, 2009). Changes in magma fO_2 may be associated with changes in either H_2O or CO_2 (Lehmann et al., 2007; Ripley and Li, 2013). For example, one way that CO_2 is added to magmas is through assimilation of carbonate material, where the principal mechanism is carbonate dissociation via the simplified reaction: $CO_2 + 2FeO \rightleftarrows CO + Fe_2O_3$ (Xue et al., 2023). Although the importance of changes to magma fO_2 on sulphide saturation at E&L cannot be currently assessed, textural evidence for mafic magma-carbonate interaction (Fig. 4i) suggests that carbonate-bearing material was likely assimilated by the magma and that contamination may have played a role in sulphide saturation. Although the carbonate that occurs interstitial to primary silicates and commonly with sulphides may be hydrothermal in origin, it is also possible that this carbonate crystallized from the magma as a result of assimilation of carbonate-rich country rock (Fig. 5e).

The simplest and most efficient way of triggering sulphide saturation in a magma is by the direct addition of sulphur, either by bulk assimilation of S-rich country rocks or selective assimilation of country-rock sulphides (Barnes and Robertson, 2019), with the former also contributing SiO_2, which serves to lower the sulphur content at sulphide saturation. Although the scale at which these processes operated at E&L is currently unknown, addition of S from country rocks is likely because: 1) the S-rich nature of the siltstones and mudstones of the Spatsizi Formation (Figs. 4n, o); 2) the occurrence of (semi-) massive sulphide orebodies near contacts with, and hosted in, sedimentary rocks of the Hazelton Group (Fig. 3); and 3) the close spatial association of semi-massive sulphides with felsic patches (Figs. 4c, h) that are consistent with localized silica addition.

6.2. Vapour-assisted transport of sulphide liquid?

Considering that assimilation of Hazelton Group sedimentary rocks may have contributed to the formation of sulphides, the occurrence of sulphides in shallow and deep portions of the E&L deposit (e.g., wehrlite from the Eastern Extensional zone; Fig. 4j), and the presence of Hazelton Group sedimentary rocks at depth (Fig. 3), some sulphide liquid may have been carried upwards through the intrusive plumbing system. Although upward transport of dense (4-5 g/cm³; Mungall and Su, 2005), low viscosity (0.01-0.1 Pa·s; Dobson et al., 2000) sulphide liquid is possible in mafic magmas, the notably lower density and fluidity of these magmas (2.7-2.9 g/cm³, 1-100 Pa·s; Williams et al., 1998) generally hinders efficient upward transport of all but the finest dispersions of sulphide liquid (Lesher, 2019). Based on experimental observations (Mungall et al., 2015), natural observations (Barnes et al., 2019, 2023; Brzozowski et al., 2023), and numerical simulations (Yao and Mungall, 2020), it has been demonstrated that upward transport of sulphide liquid can be facilitated by vapour bubbles attached to sulphide droplets (i.e., compound droplets). These compound droplets, which have been identified in other magmatic sulphide systems globally, including Norilsk (Barnes et al., 2019, 2023) and Current (Brzozowski et al., 2023), generally comprise a sulphide assemblage that has segregated into an Fe-rich portion (pyrrhotite+pentlandite) and a Cu-rich portion (chalcopyrite ±cubanite), with the latter portion being rimmed by an assemblage of silicate minerals that is finer grained than the host rock. A texturally similar style of blebby sulphide is common at E&L (Figs. 4b, 5a, d), implying that: 1) the fertile E&L magma(s) contained sufficient volatiles to become saturated, potentially because of assimilation of sedimentary country rock (e.g., Iacono-Marziano et al., 2012, 2017); 2) the magma(s) were emplaced at relatively shallow depths (low confining pressures) where volatiles could exsolve; and 3) some amount of upward transport of sulphide liquid may have occurred. If our interpretation of vapour bubbles illustrated in Figure 4b is correct, it would imply significant tilting of the E&L deposit after it formed because the core was taken from a relatively steep drill hole and the bubbles indicate tops perpendicular to the long axis of the core.

73

Geological Fieldwork 2023, British Columbia Ministry of Energy, Mines and Low Carbon Innovation, British Columbia Geological Survey Paper 2024-01

6.3. Metal remobilization?

The rocks that host the E&L deposit are pervasively altered, indicating that fluids fluxed through the mineralizing system after it had solidified. Alongside the primary silicates that were replaced by hydrous silicates, the oxides and sulphides were also altered. Several lines of textural evidence indicate that this hydrothermal activity likely remobilized metals, an understanding of which is vital given that such remobilization can have beneficial (e.g., Roby zone of Lac des Iles; Watkinson and Dunning, 1979; Hinchey and Hattori, 2005) or detrimental effects on the economic value of deposits (Holwell et al., 2017). Several factors support metal remobilization in the E&L deposit. First, given that pyrrhotite appears to have been partially to completely replaced by pyrite (Fig. 5b), as is typical of sulphide assemblages containing pyrite in these mineralizing systems (Djon and Barnes, 2012; Duran et al., 2015; Holwell et al., 2017; Brzozowski et al., 2023), Fe must have been released to the fluid and remobilized because pyrrhotite has a higher Fe content than pyrite (~62 wt.% vs. 47 wt.%). Second, the partial to complete replacement of olivine and pyroxene by sulphides (Figs. 5h, i) is strong evidence for metal remobilization. Although the Fe in this secondary sulphide assemblage could have been sourced from the primary silicates, the fact that some of these assemblages also contain chalcopyrite (Figs. 5i) and pentlandite implies that at least some of the metals were provided by the fluid that interacted with olivine and pyroxene. Third, the replacement of magnetite interstitial to ilmenite lamellae with a hydrous silicate-sulphide assemblage (Fig. 5j) indicates that metals precipitated from a hydrothermal fluid. This is because oxy-exsolution of ilmenite is a post-cumulus process that occurs at temperatures below which sulphide liquids crystallize (Buddington and Lindsley, 1964; Brzozowski et al., 2021), indicating that any sulphides present in the replacement assemblage must be hydrothermal. Fourth, some sulphides are rimmed by magnetite (Fig. 5l), which indicates S loss. Given that magnetite is unable to contain all the Cu and Ni (as well as other metals) in chalcopyrite and pentlandite (ppm vs. wt.%), respectively, these metals must have been remobilized. Finally, the occurrence of chalcopyrite, pyrrhotite, and pentlandite in late-stage veins that crosscut the E&L host rocks (Fig. 5k) implies that at least Cu, Fe, Ni, and S were remobilized by hydrothermal fluids, with other mobile trace metals likely being remobilized as well.

Given that the E&L deposit was metamorphosed at greenschist facies and that deformation is locally recorded in the sulphides (Figs. 5f, g), it is possible that sulphides were mechanically remobilized. A single sample of semi-massive sulphide exhibits textural evidence of sulphide flow, and segregation of Fe-rich and Cu-rich sulphides (Fig. 4m), indicating that some degree of mechanical remobilization could have occurred. Additionally, Vandenburg (2020) reported folded loop textures, which indicate ductile deformation. Deformation of sulphides is most prominently recorded as undulose extinction of pyrrhotite (Figs. 5g, h) and, rarely, as pyrite aggregates with flow textures in pyrrhotite-pentlandite-chalcopyrite assemblages.

Nonetheless, sulphide grains overall retain magmatic textures and do not appear to be severely deformed (Fig. 5g), suggesting minimal deformation-induced remobilization.

Taken together, it is evident that metals were remobilized by hydrothermal fluids in the E&L deposit. However, the metals that were remobilized (apart from Fe-Ni-Cu), the extent of this remobilization, and the nature of the hydrothermal fluids that caused the remobilization (e.g., deuteric vs. meteoric) remain unknown. These will be assessed in future research using bulk-rock geochemistry, in situ trace-element chemistry of sulphides, and Cu-Fe-O isotopes.

6.4. Origin of orbicular textures?

Gabbroic rocks of the E&L deposit exhibit conspicuous orbicular textures that are generally more plagioclase rich compared to the interstitial material (Figs. 4e-g). Orbicular textures have been described in a variety of rock types ranging from gabbros to granites and in a diversity of tectonic settings (Leveson, 1966). Nonetheless, the mechanism(s) by which orbicules form remains unresolved. Numerous models have been proposed, almost exclusively for those in granitic rocks, including: 1) fractional crystallization of small blebs of melt in a host magma; 2) nucleation on xenoliths; 3) mingling of compositionally distinct magmas; 4) metasomatism; and 5) liquid immiscibility (Moore and Lockwood, 1973; Sylvester, 2011; Smillie and Turnbull, 2014; Ballhaus et al., 2015; McCarthy et al., 2016; McCarthy and Müntener, 2017). Most of these models can be ruled out as having played a significant role in generating the orbicular textures at E&L. Fractional crystallization of small melt bodies can be ruled out because, although some orbicules exhibit mineralogical zonation, this is not pervasive even at the scale of a hand sample, and repetitive concentric zoning, which would be expected if each orbicule fractionally crystallized in a relatively closed system, is not observed nor was a more evolved mineral assemblage (e.g., alkali feldspar, quartz). Nucleation on xenoliths is untenable because the E&L orbicules lack xenolithic cores (Figs. 4e-g) and orbicular rocks are not restricted to the margins of the intrusion. Magma mingling can also be ruled out because the mineralogy of the orbicules at E&L is the same as that of the interstitial material, albeit the mineral abundances are different (Figs. 4e-g). Although formation of conduit-type Ni-Cu-PGE deposits generally requires input of multiple pulses of magma, these pulses are typically of similar chemical and physical composition (e.g., Shahabi Far et al., 2019), and thus will not possess sufficient contrast in physical properties (e.g., viscosity) to generate orbicules. Metasomatic reaction between magma and xenoliths can be ruled out because xenoliths of country rock material are rare at E&L and the cores of the orbicules are not xenoliths (Smillie and Turnbull, 2014).

Fluid-melt immiscibility is one of the only models of orbicule formation that has been applied to mafic-ultramafic rocks (Ballhaus et al., 2015). This model considers that all immiscible systems behave the same way and generate spheroidal textures upon exsolution, and that co-existing melts

74

Geological Fieldwork 2023, British Columbia Ministry of Energy, Mines and Low Carbon Innovation, British Columbia Geological Survey Paper 2024-01

and fluids at equilibrium are saturated in the same crystalline phases and phase compositions, and thus will crystallize to the same anhydrous minerals, but with variable proportions and grain size. Ballhaus et al. (2015) attributed the mineralogic variability to the wettability and degree of polymerization of different minerals, with neosilicates (e.g., olivine), chain silicates (e.g., pyroxene and amphibole), and oxides being transferred preferentially from melt to fluid, such that the fluid becomes more mafic, and grain size variability to faster growth rates in depolymerized fluids, such that the fluid becomes coarser grained than the melt.

The orbicules observed at E&L are similar to an immiscibility texture described by Ballhaus et al. (2015) who considered its formation to be a result of exsolution of limited amounts of water from melts during crystallization, with the two phases having a significant viscosity contrast. Accordingly, the orbicules represent the melt and the interstitial material represents the exsolved fluid (Ballhaus et al., 2015). Applied to the present example, the E&L orbicules should be relatively more felsic (e.g., contain more plagioclase) and finer grained, and the interstitial material should be relatively more mafic (e.g., contain more olivine and pyroxene) and coarser grained. This is what is observed (Figs. 4e-g). Additionally, because the orbicules that are in contact with one another along deformed boundaries retain their individual character rather than merging into a single entity (Figs. 4f, g) supports the interpretation that they represent melt rather than exsolved fluid (Ballhaus et al., 2015).

Although mineralogical and grain size zonation of orbicules, and distribution of sulphides was not described by Ballhaus et al. (2015), some E&L orbicules display a crude zonation and sulphides are generally concentrated in the interstitial material (Figs. 4e-g). If the orbicules represent melt, then the coarser grained mafic cores and finer grained felsic rims likely represent heterogeneous transfer of mafic minerals from melt to fluid (Ballhaus et al., 2015). This heterogenous transfer may have occurred for two reasons. First, mafic minerals at the rims of orbicules would have been more easily wetted by the exsolved fluid than the minerals in the cores and thus would have been more readily transferred from melt to fluid. Second, the physical movement of coarser grained minerals in the cores would have been impeded by the crystal mush, preventing transfer. With respect to the sulphides, because they are generally concentrated in the interstitial material implies that sulphide liquid, which exsolved from the silicate melt, was preferentially transferred to the exsolved fluid, consistent with the low degree of polymerization of sulphide liquids. The occurrence of small volumes of sulphide within the cores of orbicules (Fig. 4f) may be attributed to the impeded movement of mafic minerals described above.

In summary, we conclude that the magmas from which the E&L deposit crystallized may have contained sufficient H_2O to become saturated and exsolve a hydrous fluid at depth. The lack of these orbicular textures in the barren Nickel mountain gabbro may indicate that the fertile magmas from which the mineralized E&L stock crystallized were more hydrous. However, it remains unclear if such possible fluid-rich magmas played a role in generating the mineralization and in altering the host rocks (i.e., auto-hydrothermal alteration).

7. Conclusion

The mafic-ultramafic rocks of the E&L Ni-Cu-PGE sulphide deposit that intruded sedimentary rocks of the Spatsizi Formation and the Nickel mountain gabbro exhibit a variety of macro- and micro-scale textures that provide insights into potential mechanisms that may have formed and modified the deposit. The spatial association of carbonates with sulphides and the occurrence of sulphides in felsic patches in the mafic host rock suggest that assimilation of country rock material contributed to the sulphide saturation history of the E&L magma. The occurrence of compound droplets (sulphide+hydrous silicates/vapour bubbles) is inferred to represent vapour saturation in the magma, which likely assisted in the upward transport of sulphide liquid. The widespread mineralogical and textural evidence indicative of sulphide remobilization (pyrite after pyrrhotite, sulphides after olivine, pyroxene, and magnetite, sulphides in veins, magnetite after sulphides) indicates that metals were remobilized throughout the E&L deposit, although the extent of remobilization remains unclear. Although sulphides are deformed, they retain magmatic textures, suggesting minimal deformation-induced remobilization. The occurrence of orbicules in many of the E&L gabbros may indicate H_2O saturation of the magma and fluid immiscibility, with the orbicules representing the silicate melt and the interstitial material representing the exsolved hydrous fluid. Planned future work will use bulk-rock geochemistry, Sr-Nd-S-C-O ±Cu-Fe isotopes, and sulphide trace-element chemistry to more fully document the processes that formed and modified the E&L deposit.

References cited

Acosta-Góngora, P., Pehrsson, S.J., Sandeman, H., Martel, E., and Peterson, T., 2018. The Ferguson Lake deposit: an example of Ni-Cu-Co-PGE mineralization emplaced in a back-arc basin setting? Canadian Journal of Earth Sciences, 55, 958-979.

Alldrick D.J., Brown D.A., Harakal J.E., Mortensen J.K., and Armstrong R.L., 1987. Geochronology of the Stewart Mining Camp (104B/1). In: Geological Fieldwork 1986. British Columbia Ministry of Energy, Mines and Petroleum Resources, British Columbia Geological Survey Paper 1987-01, pp. 81-92.

Arndt, N., Lesher, C.M., and Czamanske, G.K., 2005. Mantle-derived magmas and magmatic Ni-Cu-(PGE) deposits. In: Hedenquist, J.W., Thompson, J.F.H., Goldfarb, R.J., Richards, J.P., (Eds.), Economic Geology, 100th Anniversary Volume, pp. 5-24.

Ballhaus, C., Fonseca, R.O.C., Münker, C., Kirchenbaur, M., and Zirner, A., 2015. Spheroidal textures in igneous rocks - Textural

75

Geological Fieldwork 2023, British Columbia Ministry of Energy, Mines and Low Carbon Innovation, British Columbia Geological Survey Paper 2024-01

consequences of H$_2$O saturation in basaltic melts. Geochimica et Cosmochimica Acta, 167, 241-252.

Barnes, S.J., and Robertson, J.C., 2019. Time scales and length scales in magma flow pathways and the origin of magmatic Ni-Cu-PGE ore deposits. Geoscience Frontiers, 10, 77-87.

Barnes, S.J., Cruden, A.R., Arndt, N., and Saumur, B.M., 2015. The mineral system approach applied to magmatic Ni-Cu-PGE sulphide deposits. Ore Geology Reviews, 76, 296-316.

Barnes, S.J., Le Vaillant, M., Godel, B., and Lesher, C.M., 2019. Droplets and bubbles: Solidification of sulphide-rich vapour-saturated orthocumulates in the Norilsk-Talnakh Ni-Cu-PGE Ore-bearing Intrusions. Journal of Petrology, 60, 269-300.

Barnes, S.J., Yudovskaya, M.A., Iacono-Marziano, G., Vaillant, M.L., Schoneveld, L.E., and Cruden, A.R., 2023. Role of volatiles in intrusion emplacement and sulfide deposition in the supergiant Norilsk-Talnakh Ni-Cu-PGE ore deposits. Geology, 51, 1027-1032.

British Columbia Geological Survey, 2023. The Golden Triangle of northwestern British Columbia. British Columbia Ministry of Energy, Mines and Petroleum Resources, British Columbia Geological Survey Information Circular 2023-05, 6 p.

Brzozowski, M.J., Samson, I.M., Gagnon, J.E., Good, D.J., and Linnen, R.L., 2020. On the mechanisms for low-sulfide, high-platinum group element and high-sulfide, low-platinum group element mineralization in the Eastern gabbro, Coldwell Complex, Canada: Evidence from textural associations, S/Se values, and platinum group element concentrations of base metal sulfides. Economic Geology, 115, 355-384.

Brzozowski, M.J., Samson, I.M., Gagnon, J.E., Linnen, R.L., and Good, D.J., 2021. Effects of fluid-induced oxidation on the composition of Fe-Ti oxides in the Eastern Gabbro, Coldwell Complex, Canada: implications for the application of Fe-Ti oxides to petrogenesis and mineral exploration. Mineralium Deposita, 56, 601-618.

Brzozowski, M.J., Hollings, P., Heggie, G., MacTavish, A., Wilton, D., and Evans-Lamswood, D., 2023. Characterizing the supra- and subsolidus processes that generated the Current PGE-Cu-Ni deposit, Thunder Bay North Intrusive Complex, Canada: insights from trace elements and multiple S isotopes of sulfides. Mineralium Deposita, 58, 1559-1581.

Buddington, A.F., and Lindsley, D.H., 1964. Iron-titanium oxide minerals and synthetic equivalents. Journal of Petrology, 5, 310-357.

Campbell, I.H., and Naldrett, A.J., 1979. The influence of silicate: sulfide ratios on the geochemistry of magnetic sulfides. Economic Geology, 74, 1503-1506.

Colpron, M., 2020. Yukon terranes-A digital atlas of terranes for the northern Cordillera. Yukon Geological Survey. https://data.geology.gov.yk.ca/Compilation/2#InfoTab>

Craig, J.R., 1973. Pyrite-pentlandite assemblages and other low temperature relations in the Fe-Ni-S system. American Journal of Science, 273-A, 496-510.

Ding, X., Ripley, E.M., and Li, C., 2011. PGE geochemistry of the Eagle Ni-Cu-(PGE) deposit, Upper Michigan: constraints on ore genesis in a dynamic magma conduit. Mineralium Deposita, 47, 89-104.

Djon, M.L.N., and Barnes, S.J., 2012. Changes in sulfides and platinum-group minerals with the degree of alteration in the Roby, Twilight, and High Grade Zones of the Lac des Iles Complex, Ontario, Canada. Mineralium Deposita, 47, 875-896.

Dobson, D.P., Crichton, W.A., Vočadlo, L., Jones, A.P., Wang, Y., Uchida, T., Rivers, M., Sutton, S., and Brodholt, J.P., 2000. In situ measurement of viscosity of liquids in the Fe-FeS system at high pressures and temperatures. American Mineralogist, 85, 1838-1842.

Duran, C.J., Barnes, S-J., and Corkery, J.T., 2015. Chalcophile and platinum-group element distribution in pyrites from the sulfide-rich pods of the Lac des Iles Pd deposits, Western Ontario, Canada: Implications for post-cumulus re-equilibration of the ore and the use of pyrite compositions in exploration. Journal of Geochemical Exploration, 158, 223-242.

Evans-Lamswood, D.M., Butt, D.P., Jackson, R.S., Lee, D.V., Muggridge, M.G., and Wheeler, R.I., 2000. Physical Controls Associated with the Distribution of Sulfides in the Voisey's Bay Ni-Cu-Co Deposit, Labrador. Economic Geology, 95, 22.

Gagnon, J.-F., Barresi, T., Waldron, J.W.F., Nelson, J.L., Poulton, T.P., and Cordey, F., 2012. Stratigraphy of the upper Hazelton Group and the Jurassic evolution of the Stikine terrane, British Columbia. Canadian Journal of Earth Sciences, 49, 1027-1052.

Gao, J.-F., Zhou, M.-F., Lightfoot, P.C., Wang, C.Y., Qi, L., and Sun, M., 2013. Sulfide Saturation and Magma Emplacement in the Formation of the Permian Huangshandong Ni-Cu Sulfide Deposit, Xinjiang, Northwestern China. Economic Geology, 108, 1833-1848.

Hancock, K.D., 1990. Geology of Nickel Mountain and the E&L nickel-copper prospect (104B/10E). In: Geological Fieldwork 1989, British Columbia Ministry of Energy, Mines and Petroleum Resources, British Columbia Geological Survey Paper 1990-1, pp. 337-341.

Hanson, J., Lightfoot, P.C., and Goldie, R., 2022. Nickel mountain and Casper exploration: 2022 corporate presentation. Garibaldi Resources Corp. <https://garibaldiresources.com/site/assets/files/3966/ggi-investor-presentation-july-2022.pdf>. Accessed November 17, 2023.

Hinchey, J.G., and Hattori, K.H., 2005. Magmatic mineralization and hydrothermal enrichment of the High Grade Zone at the Lac des Iles palladium mine, northern Ontario, Canada. Mineralium Deposita, 40, 13-23.

Holwell, D.A., Adeyemi, Z., Ward, L.A., Smith, D.J., Graham, S.D., McDonald, I., and Smith, J.W., 2017. Low temperature alteration of magmatic Ni-Cu-PGE sulfides as a source for hydrothermal Ni and PGE ores: A quantitative approach using automated mineralogy. Ore Geology Reviews, 91, 718-740.

Iacono-Marziano, G., Marecal, V., Pirre, M., Gaillard, F., Arteta, J., Scaillet, B., and Arndt, N.T., 2012. Gas emissions due to magma-sediment interactions during flood magmatism at the Siberian Traps: Gas dispersion and environmental consequences. Earth and Planetary Science Letters, 357-358, 308-318.

Iacono-Marziano, G., Ferraina, C., Gaillard, F., Di Carlo, I., and Arndt, N.T., 2017. Assimilation of sulfate and carbonaceous rocks: Experimental study, thermodynamic modeling and application to the Noril'sk-Talnakh region (Russia). Ore Geology Reviews, 90, 399-413.

Jackson-Brown, S., Scoates, J.S., Nixon, G.T., and Ames, D.E., 2014. Mineralogy of sulphide, arsenide, and platinum group minerals from the DJ/DB Zone of the Turnagain Alaskan-type ultramafic intrusion, north-central British Columbia. In: Geological Fieldwork 2013, British Columbia Ministry of Energy and Mines, British Columbia Geological Survey Paper 2014-1, pp. 157-168.

Jugo, P.J., 2004. An experimental study of the sulfur content in basaltic melts saturated with immiscible sulfide or sulfate liquids at 1300°C and 1.0 GPa. Journal of Petrology, 46, 783-798.

Jugo, P.J., 2009. Sulfur content at sulfide saturation in oxidized magmas. Geology, 37, 415-418.

Kellerud, G., Yund, R.A., and Moh, G.H., 1969. Phase relations in the Cu-Fe-S, Cu-Ni-S, and Fe-Ni-S systems. Economic Geology Monograph, 4, 323.

Lee, I., and Ripley, E.M., 1995. Genesis of Cu-Ni sulfide mineralization in the South Kawishiwi intrusions, Spruce Road area, Duluth Complex, Minnesota. The Canadian Mineralogist, 33, 723-743.

Lehmann, J., Arndt, N., Windley, B., Zhou, M.-F., Wang, C.Y., and Harris, C., 2007. Field Relationships and Geochemical Constraints on the Emplacement of the Jinchuan Intrusion and its Ni-Cu-PGE

76

Geological Fieldwork 2023, British Columbia Ministry of Energy, Mines and Low Carbon Innovation, British Columbia Geological Survey Paper 2024-01

Sulfide Deposit, Gansu, China. Economic Geology, 102, 75-94.

Lesher, C.M., 2019. Up, down, or sideways: emplacement of magmatic Fe-Ni-Cu-PGE sulfide melts in large igneous provinces. Canadian Journal of Earth Sciences, 56, 756-773.

Leveson, D.J., 1966. Orbicular Rocks: A Review. Geological Society of America Bulletin, 77, 409-426.

Li, X.H., Su, L., Chung, S.-L., Li, Z.X., Liu, Y., Song, B., and Liu, D.Y., 2005. Formation of the Jinchuan ultramafic intrusion and the world's third largest Ni-Cu sulfide deposit: Associated with the ~825 Ma south China mantle plume? Geochemistry, Geophysics, Geosystems, 6, 1-16.

Lightfoot, P.C., Keays, R.R., Evans-Lamswood, D., and Wheeler, R., 2012. S saturation history of Nain Plutonic Suite mafic intrusions: origin of the Voisey's Bay Ni-Cu-Co sulfide deposit, Labrador, Canada. Mineralium Deposita, 47, 23-50.

Manor, M.J., Scoates, J.S., Nixon, G.T., and Ames, D.E., 2014. Platinum-group mineralogy of the Giant Mascot Ni-Cu-PGE deposit, Hope, B.C. In: Geological Fieldwork 2013, British Columbia Ministry of Energy and Mines, British Columbia Geological Survey Paper 2014-1, pp. 141-156.

Manor, M.J., Scoates, J.S., Nixon, G.T., and Ames, D.E., 2016. The Giant Mascot Ni-Cu-PGE deposit, British Columbia: Mineralized donduits in a convergent margin tectonic setting. Economic Geology, 111, 57-87.

Mao, Y.-J., Qin, K.-Z., Li, C., and Tang, D.-M., 2015. A modified genetic model for the Huangshandong magmatic sulfide deposit in the Central Asian Orogenic Belt, Xinjiang, western China. Mineralium Deposita, 50, 65-82.

Mavrogenes, J.A., and O'Neill, H.S.C., 1999. The relative effects of pressure, temperature and oxygen fugacity on the solubility of sulfide in mafic magmas. Geochimica et Cosmochimica Acta, 63, 1173-1180.

McCarthy, A., and Müntener, O., 2017. Mineral growth in melt conduits as a mechanism for igneous layering in shallow arc plutons: mineral chemistry of Fisher Lake orbicules and comb layers (Sierra Nevada, USA). Contributions to Mineralogy and Petrology, 172, 55.

McCarthy, A., Müntener, O., Bouvier, A.-S., and Baumgartner, L., 2016. Melt Extraction Zones in Shallow Arc Plutons: Insights from Fisher Lake Orbicules (Sierra Nevada, Western USA). Journal of Petrology, 57, 2011-2052.

Milidragovic, D., Nixon, G.T., Scoates, J.S., Nott, J.A., and Spence, D.W., 2021. Redox-controlled chalcophile element geochemistry of the Polaris Alaskan-type mafic-ultramafic complex, British Columbia, Canada. The Canadian Mineralogist, 59, 1627-1660.

Milidragovic, D., Nott, J.A, Spence, D.W., Schumann, D., Scoates, J.S., Nixon, G.T., and Stern, R.A., 2023. Sulfate recycling at subduction zones indicated by sulfur isotope systematics of Mesozoic ultramafic island arc cumulates in the North American Cordillera. Earth and Planetary Science Letters, 620, article 118337. <https://doi.org/10.1016/j.epsl.2023.118337>

Moore, J.G., and Lockwood, J.P., 1973. Origin of comb layering and orbicular structure, Sierra Nevada Batholith, California. Geological Society of America Bulletin, 84, 1-19.

Mudd, G.M., and Jowitt, S.M., 2014. A detailed assessment of global nickel resource trends and endowments. Economic Geology, 109, 1813-1841.

Mudd, G.M., and Jowitt, S.M., 2022. The new century for nickel resources, reserves, and mining: Reassessing the sustainability of the devil's metal. Economic Geology, 117, 1961-1983.

Mudd, G.M., Jowitt, S.M., and Werner, T.T., 2018. Global platinum group element resources, reserves and mining - A critical assessment. Science of The Total Environment, 622-623, 614-625.

Mungall, J.E., 2014. Geochemistry of magmatic ore deposits. In: Treatise on Geochemistry, Elsevier, pp. 195-218.

Mungall, J., and Su, S., 2005. Interfacial tension between magmatic sulfide and silicate liquids: Constraints on kinetics of sulfide liquation and sulfide migration through silicate rocks. Earth and Planetary Science Letters, 234, 135-149.

Mungall, J.E., Brenan, J.M., Godel, B., Barnes, S.J., and Gaillard, F., 2015. Transport of metals and sulphur in magmas by flotation of sulphide melt on vapour bubbles. Nature Geoscience, 8, 216-219.

Naldrett, A.J., 1989. Introduction: Magmatic deposits associated with mafic rocks. In: Whitney, J. A., Naldrett, A.J., (Eds.), Ore Deposition Associated with Magmas. Society of Economic Geologists, 4, pp. 1-3.

Naldrett, A.J., 1992. A model for the Ni-Cu-PGE ores of the Noril'sk region and its application to other areas of flood basalt. Economic Geology, 87, 1945-1962.

Naldrett, A.J., 1999. World-class Ni-Cu-PGE deposits: key factors in their genesis. Mineralium Deposita, 34, 227-240.

Naldrett, A.J., 2010. From the mantle to the bank: The life of a Ni-Cu-(PGE) sulfide deposit. South African Journal of Geology, 113, 1-32.

Naldrett, A.J., Cragi, J.R., and Kellurud, G., 1967. The central portion of the Fe-Ni-S system and its bearing on pentlandite exsolution in iron-nickel sulfide ores. Economic Geology, 62, 826-847.

Nelson, J.L., Diakow L., van Staal, C., and Chipley, D., 2013. Ordovician volcanogenic sulphides in the southern Alexander terrane, coastal NW British Columbia: geology, Pb isotopic signature, and a case for correlation with Appalachian and Scandinavian deposits. In: Geological Fieldwork 2012, British Columbia Ministry of Energy, Mines and Natural Gas, British Columbia Geological Survey Paper 2013-1, pp. 13-33.

Nelson, J., Waldron, J., van Straaten, B., Zagorevski, A., and Rees, C., 2018. Revised stratigraphy of the Hazelton Group in the Iskut River region, northwestern British Columbia. In: Geological Fieldwork 2017. British Columbia Ministry of Energy, Mines and Petroleum Resources, British Columbia Geological Survey Paper 2018-01, pp. 15-38.

Nelson, J.L., van Straaten, B., and Friedman R., 2022. Latest Triassic-Early Jurassic Stikine-Yukon-Tanana terrane collision and the onset of accretion in the Canadian Cordillera: Insights from Hazelton Group detrital zircon provenance and arc-back-arc configuration. Geosphere, 18, 670-696.

Nixon, G.T., Manor, M.J., and Scoates, J.S., 2018. Cu-PGE Sulphide mineralization in the Tulameen Alaskan-type Intrusion: Analogue for Cu-PGE reefs in layered Intrusions? British Columbia Ministry of Energy, Mines and Petroleum Resources, British Columbia Geological GeoFile 2018-02.

Nixon, G.T., Scheel, J.E., Scoates, J.S., Friedman, R.M., Wall, C.J., Gabites, J., and Jackson-Brown, S., 2020. Syn-accretionary multistage assembly of an Early Jurassic Alaskan-type intrusion in the Canadian Cordillera: U-Pb and $^{40}Ar/^{39}Ar$ geochronology of the Turnagain ultramafic-mafic intrusive complex, Yukon-Tanana terrane. Canadian Journal of Earth Sciences, 57, 575-600.

O'Neill, H.S.C., and Mavrogenes, J.A., 2002. The Sulfide Capacity and the Sulfur Content at Sulfide Saturation of Silicate Melts at 1400°C and 1 bar. 43, 39.

Piña, R., Romeo, I., Ortega, L., Lunar, R., Capote, R., Gervilla, F., Tejero, R., and Quesada, C., 2010. Origin and emplacement of the Aguablanca magmatic Ni-Cu-(PGE) sulfide deposit, SW Iberia: A multidisciplinary approach. Geological Society of America Bulletin, 122, 915-925.

Piña, R., Gervilla, F., Barnes, S.-J., Oberthür, T., and Lunar, R., 2016. Platinum-group element concentrations in pyrite from the Main Sulfide Zone of the Great Dyke of Zimbabwe. Mineralium Deposita, 51, 853-872.

Ripley, E., and Li, C., 2011. A review of conduit-related Ni-Cu-(PGE) sulfide mineralization at the Voisey's Bay Deposit, Labrador, and the Eagle Deposit, northern Michigan. Reviews in Economic Geology, 17, 181-197.

Ripley, E.M., and Li, C., 2013. Sulfide saturation in mafic magmas: is external sulfur required for magmatic Ni-Cu-(PGE) ore genesis? Economic Geology, 108, 45-58.

Sappin, A.-A., Constantin, M., Clark, T., and Van Breemen, O., 2009. Geochemistry, geochronology, and geodynamic setting of Ni-Cu±PGE mineral prospects hosted by mafic and ultramafic intrusions in the Portneuf-Mauricie Domain, Grenville Province, Quebec. Canadian Journal of Earth Sciences, 46, 331-353.

Scheel, J.E., 2004. Age and origin of the Turnagain Alaskan-type intrusion and associated Ni-sulphide mineralization, north-central British Columbia, Canada. Unpublished MSc. thesis, University of Alberta, 201 p.

Shahabi Far, M., Samson, I.M., Gagnon, J.E., Good, D.J., Linnen, R.L., and Ames, D., 2019. Evolution of a conduit system at the Marathon PGE-Cu deposit: Insights from silicate mineral Textures and Chemistry. Journal of Petrology, 60, 1-3.

Smillie, R.W., and Turnbull, R.E., 2014. Field and petrographical insight into the formation of orbicular granitoids from the Bonney Pluton, southern Victoria Land, Antarctica. Geological Magazine, 151, 534-549.

Stifter, E.C., Ripley, E.M., and Li, C., 2016. Os and S isotope studies of ultramafic rocks in the Duke Island Complex, Alaska: variable degrees of crustal contamination of magmas in an arc setting and implications for Ni-Cu-PGE sulfide mineralization. Mineralium Deposita, 51, 903-918.

Sun, T., Tan, S.-C., Yang, S.-H., Hanski, E., Zhou, J.-X., Li, H.-T., Zhang, A.-P., Li, W.-T., and Zhou, Y.-G., 2021. Early Permian subduction-related Ni-Cu sulfide mineralization in the Central Asian Orogenic Belt: A case of the Halatumiao deposit. Ore Geology Reviews, 130, article 103974. <https://doi.org/10.1016/j.oregeorev.2020.103974>

Sylvester, A.G., 2011. The nature and polygenetic origin of orbicular granodiorite in the Lower Castle Creek pluton, northern Sierra Nevada batholith, California. Geosphere, 7, 1134-1142.

Thakurta, J., Ripley, E.M., and Li, C., 2008. Geochemical constraints on the origin of sulfide mineralization in the Duke Island Complex, southeastern Alaska. Geochemistry, Geophysics, Geosystems, 9, 1-34.

Vandenburg, E.D.J., 2020. The E&L magmatic Ni-Cu-(PGE) deposit, northwestern British Columbia: Preliminary sulfide petrology, platinum-group element mineralogy and lead isotope systematics. Unpublished B.Sc. thesis, The University of British Columbia, 194 p.

Wang, S., Wu, C., Muhtar, M.N., Lei, R., and Brzozowski, M.J., 2021. Mobilization of ore-forming metals during post-magmatic hydrothermal overprinting of the Huangshandong Ni-Cu sulfide deposit, Eastern Tianshan, NW China. Ore Geology Reviews, 137, article 104315. <https://doi.org/10.1016/j.oregeorev.2021.104315>

Watkinson, D.H., and Dunning, G., 1979. Geology and platinum-group mineralization, Lac-des-Iles Complex, northwestern Ontario. Canadian Mineralogist, 17, 453-462.

Williams, D.A., Kerr, R.C., and Lesher, C.M., 1998. Emplacement and erosion by Archean komatiite lava flows at Kambalda: Revisited. Journal of Geophysical Research: Solid Earth, 103, 27533-27549.

Xue, S., Wang, Q., Wang, Y., Song, W., and Deng, J., 2023. The roles of various types of crustal contamination in the genesis of the Jinchuan magmatic Ni-Cu-PGE deposit: New mineralogical and C-S-Sr-Nd isotope constraints. Economic Geology. <https://doi.org/10.5382/econgeo.5017>

Yao, Z., and Mungall, J.E., 2020. Flotation mechanism of sulphide melt on vapour bubbles in partially molten magmatic systems. Earth and Planetary Science Letters, 542, article 116298. <https://doi.org/10.1016/j.epsl.2020.116298>

Zhang, A., Sun, T., Zhao, Z., Zhou, J., Li, W., Qi, Q., and Wei, X., 2021. Genesis of the Neoarchean subduction-related Taoke Ni-Cu-PGE sulphide deposit in the North China Craton: Constraints from Os-S isotopes and PGE geochemistry. Geological Journal, 56, 4888-4903.